5. Dendritic core-multishell architectures with PAMAM core

5.1. Introduction

PAMAM[33-35] dendrimers are one of the most commonly used commercially available perfect polymers.[10,23,51] Numerous applications of PAMAM were described in the literature including drug[22,50,351] and gene[47,51] delivery, the use as a diagnostic contrast agents[9,20] and others.[5,108,111] Several core-shell architectures with PAMAM dendrimers ([G2-G5]) as cores were also reported including PEG-PAMAM conjugates.[23,85,87,130,350,351] In none of these scientific works an aggregation of the core-shell structures was mentioned as the crucial factor for host-guest interactions.

The goal of this part of the work was to synthesize core-multishell architectures with the PAMAM dendrimer as a core and compare their properties to the ones of liposome-like structures based on hyperbranched polymers. Especially the aggregation phenomenon of the core-multishell structures was investigated. This was important to answer the question if the formation of supramolecular aggregates only appears for hyperbranched based nanotransporters, or if it can be expanded to all types of liposome-like structures.

5.2. Synthesis of core-shell architecture with PAMAM core

In order to obtain novel PAMAM core-multishell architectures the usual three-step synthesis was applied based on the synthesis of nanotransporters with PEI core. The synthesis and activation of the amphiphilic shell precursor was already presented in chapter 3.2. In the final step the activated $mPEG_xC_{18}ONSu$ was coupled to the PAMAM [G5] dendrimer (Scheme 16). The product was purified by dialysys in MeOH. Two different PAMAM based nanotransporters were synthesized: $PAMAM[G5](C_{18}mPEG_6)_{1.0}$ and $PAMAM[G5](C_{18}mPEG_6)_{1.0}$. In both polymers C_{18} aliphatic chain was used as the inner domain. The outer shell was composed from $mPEG_6$ or $mPEG_{14}$.

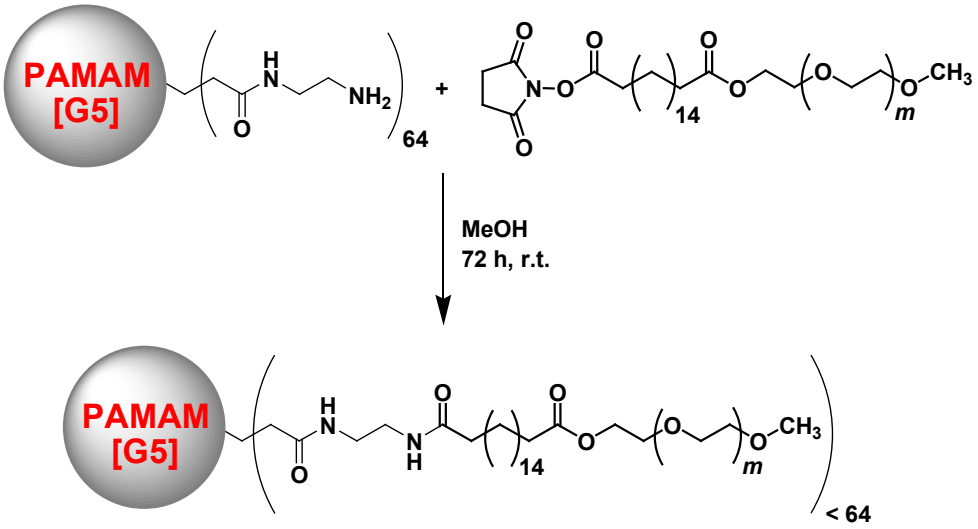

Scheme 16. Final step of the PAMAM based nanotransporters synthesis. Reactions were performed in MeOH for 72 h at r.t.. Two different polymers PAMAM[G5](C_{18}mPEG$_{m+1}$)$_{1.0}$ were obtained with *m* = 5 (mPEG$_6$) or 13 (mPEG$_{14}$). The functionalization of the PAMAM core is DF_A = 1.0.

The determination of the degree of functionalization from ^{1}H NMR spectra was difficult for core-multishell architectures with PAMAM core. The signals from the PAMAM core overlap in the range of 2.10 – 2.90 ppm with the C_{18} protons and in the range of 3.10 – 3.80 ppm with the mPEG protons. Thus the calculation of the degree of functionalization from ^{1}H NMR posses a big error (Figure 46). Therefore, the DF was calculated from the stoichiometrical amounts of PAMAM [G5] dendrimer and (C_{18}mPEG)-ONSu applied for the synthesis.

The obtained polymers were soluble in water and organic solvents ranging from toluene to water. However, the dissolution in aqueous media was slower for the nanotransporters with PAMAM core in comparison to the PEI and PG-amine based polymers.

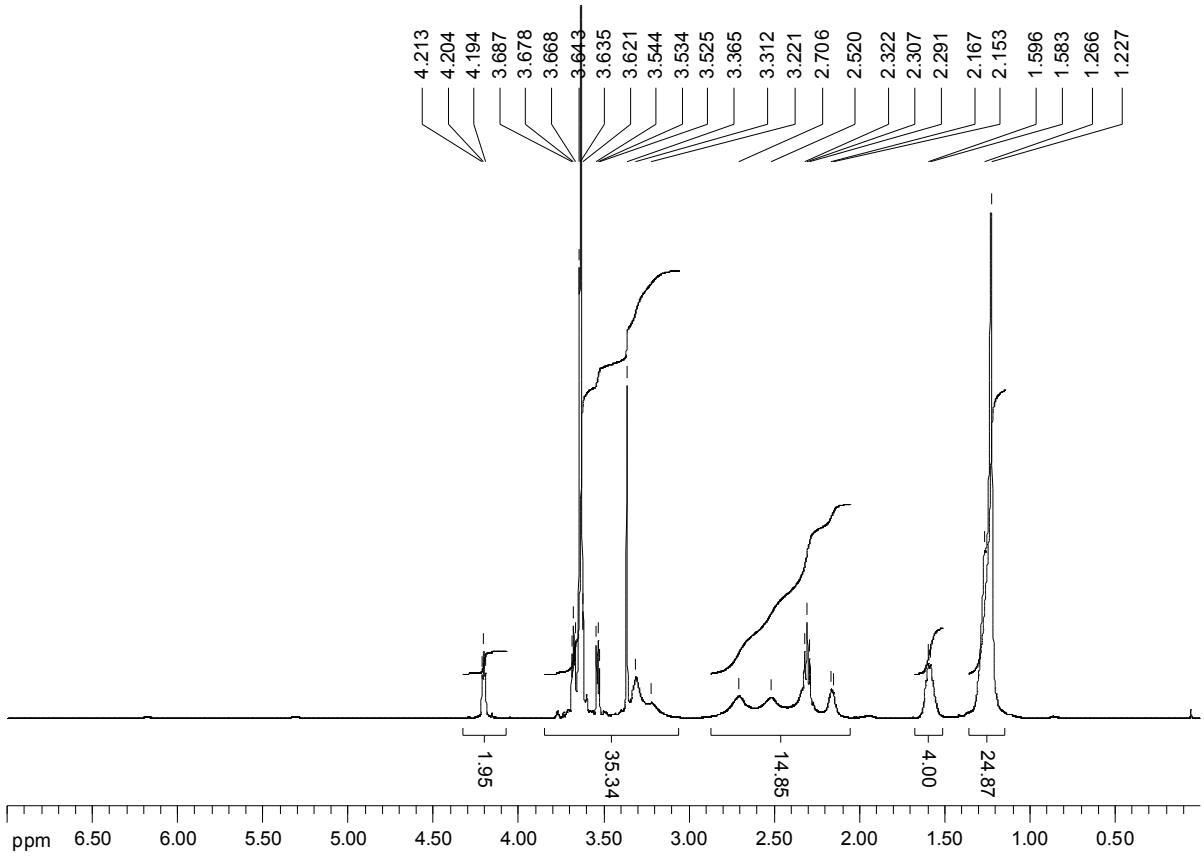

Figure 46. ^{1}H NMR spectra of PAMAM[G5](C_{18}mPEG$_6$)$_{1.0}$ in $CDCl_3$. The peaks: 1.10 – 1.35 ppm, 1.50 – 1.70 ppm, 2.10 – 2.20 ppm, and 2.25 – 2.35 ppm belong to the protons from aliphatic chain. The broad overlapping peaks: 2.20 – 2.40 ppm , 2.40 – 2.60 ppm, 2.60 – 2.75 ppm, and 3.10 – 3.40 ppm belong to the protons from PAMAM core. Singlet at 3.37 ppm, multiplets at 3.55 – 3.70 ppm and triplet at 4.20 ppm belong to protons from mPEG shell.

5.3. Determination of the transport capacity for PAMAM based core-multishell architectures

The transport capacity of the PAMAM[G5] dendrimer based polymers was determined with the solid-liquid extraction method under standard conditions (chapter 3.4). The TC was tested with congo red and rose bengal in chloroform and with nile red and β-carotene in aqueous media. The concentration of the polymers was 0.5 g l^{-1} (9.26×10^{-6} M for PAMAM[G5](C_{18}mPEG$_6$)$_{1.0}$ and 6.25×10^{-6} M for PAMAM[G5](C_{18}mPEG$_6$)$_{1.0}$). The samples were stirred for 24 h at r.t. and the resulting suspensions were filtrated *via* 0.45 μm PTFE filters. Results are summarized in Table 12.

Table 12. Transport capacity and relative transport capacity of core-multishell architectures with PAMAM core for congo red, rose bengal, nile red, and β-carotene.

Polymer	congo red		rose bengal		nile red		β-carotene	
	$TC^{[a]}$	$TC_{rel}^{[b]}$	$TC^{[a]}$	$TC_{rel}^{[b]}$	$TC^{[a]}$	$TC_{rel}^{[b]}$	$TC^{[a]}$	$TC_{rel}^{[b]}$
PAMAM(C_{18}mPEG$_6$)$_{1.0}$ M_n [g mol^{-1}] = 54000	6.90	89.0	2.56	49.7	0.88	5.22	0.84	8.32
PAMAM(C_{18}mPEG$_{14}$)$_{1.0}$ M_n [g mol^{-1}] = 80000	13.30	115.8	3.59	47.1	0.90	3.53	1.26	8.48

Concentration of polymers = 0.5 g l^{-1} (9.26×10^{-6} M for PAMAM[G5](C_{18}mPEG$_6$)$_{1.0}$ and 6.25×10^{-6} M for PAMAM[G5](C_{18}mPEG$_6$)$_{1.0}$). M_n = molecular weight of polymer calculated from stoichiometrical amounts of PAMAM and mPEG-C_{18}-ONSu applied; [a] transport capacity in mol_{guest} per mol_{host} ratio (n_{guest} / n_{host}); [b] relative transport capacity in mg guest per g polymer; TC error is < 15 %.

The encapsulation experiments revealed universal transport abilities of PAMAM liposome-like polymers for polar and nonpolar molecules. With the prolongation of the mPEG chain an increase of the TC was observed independent of the polarity of the guest molecules. The improvement was in the range of 1.4 – 1.9 times for polar molecules and β-carotene (no improvement for nile red was observed). This is in a good agreement with results obtained for core-multishell systems with hyperbranched polymers as a core. The transport capacity and relative transport capacity results for nile red and β-carotene showed similar values as observed for PEI nanotransporters. Surprisingly good values of TC and TC_{rel} were obtained for congo red, of which PAMAM[G5](C_{18}mPEG$_6$)$_{1.0}$ encapsulates more than 13 guest molecules per polymer (TC_{rel} = 116 mg of dye per gram of polymer).

The transport capacity-polymer concentration dependency test was performed to confirm that aggregation of polymers is necessary for host-guest interactions. PAMAM[G5](C_{18}mPEG$_6$)$_{1.0}$ was dissolved in chloroform and as a transport indicator congo red was used. The investigated concentration ranged from 0.0125 – 0.80 g l^{-1} (2.31×10^{-7} M - 1.48×10^{-5} M) with an additional focus on the threshold concentration 0.1 g l^{-1} (1.85×10^{-5} M) (Figure 47).

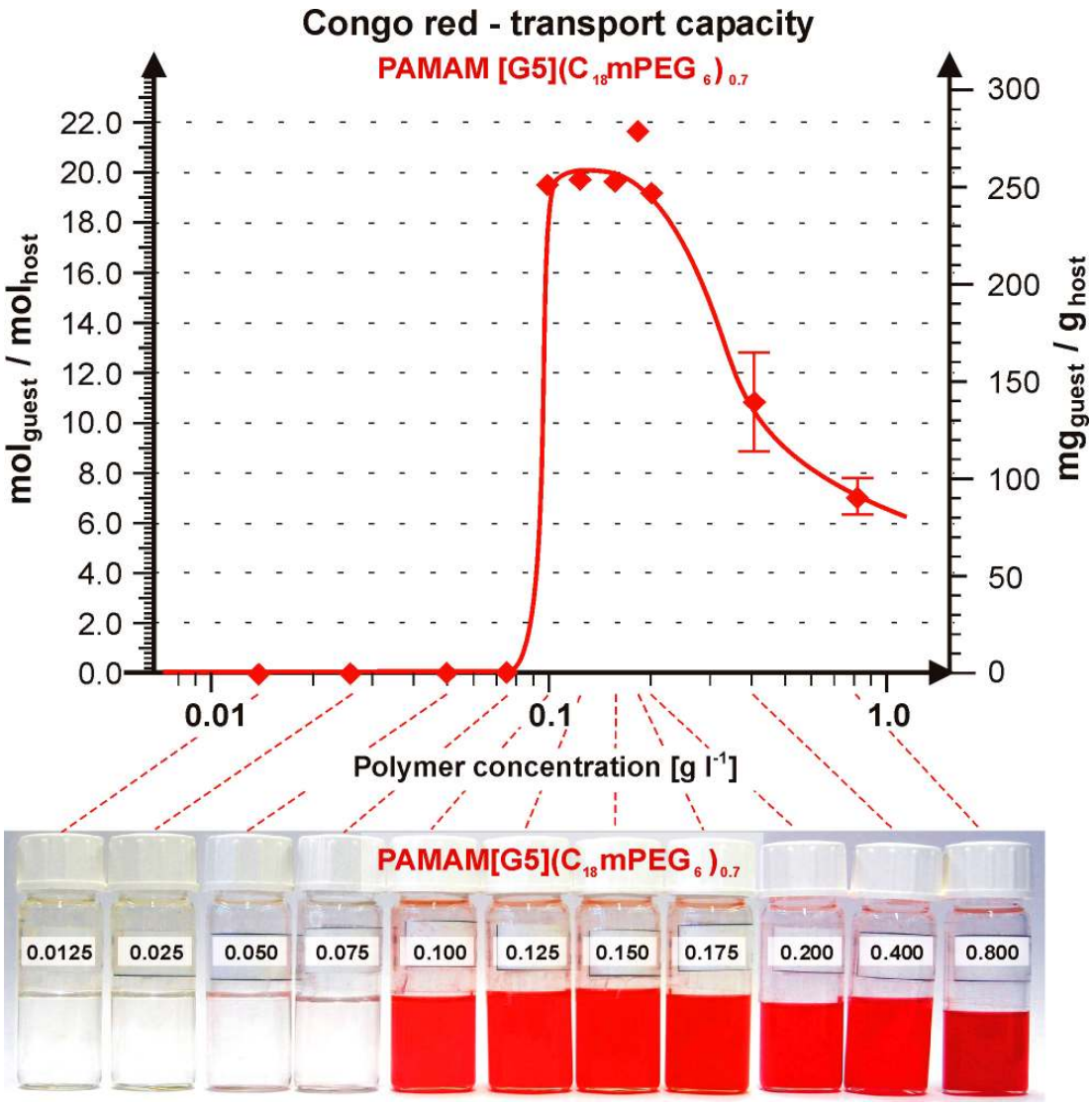

Figure 47. Influence of the polymer concentration on the transport capacity of PAMAM[G5](C_{18}mPEG$_6$)$_{0.6}$ (♦)for congo red in chloroform. The insert visualizes the congo red transport at different polymer concentrations with an increase of the polymer concentration from left to right.

The experiment revealed a nonlinear transport behavior with an extremely clear CAC located at concentration of 0.10 g l^{-1}. The difference between the aggregated and nonaggregated polymers appeared with an increase of the concentration by 0.025 g l^{-1}. This is equal to a change of 4.63×10^{-7} M (!). The increase of the TC was significant, from 0 to around 19.5 dye molecules per polymer. This is equal to a loading of the nanotransporter with approximately 250 mg / g. A further increase of the polymer concentration to the range of 0.10 – 0.20 g l^{-1} did not effect the transport capacity. For all samples the TC was almost identical. Only the sample with the concentration 0.175 g l^{-1} revealed 10 % higher transport. Between concentrations of 0.20 and 0.80 g l^{-1} a decrease of the TC was observed. The drop was significant and reduced the encapsulation ability by 2.8 times (to TC = 6.9 at 0.80 g l^{-1}). Experiments performed for PAMAM[G5](C_{18}mPEG$_6$)$_{1.0}$ showed an almost identical transport

capacity profile, although the CAC point was located at 0.20 g l^{-1}. The formation of supramolecular aggregates was confirmed by DLS.

In conclusion, core-multishell architectures with the PAMAM dendrimer as a core present identical properties compared to liposome-like polymers based on hyperbranched cores (PEI and PG-amine). Moreover, the critical aggregation concentration was clearly characterized with a resolution of 4.63×10^{-7} M.